

MODELLING AND EXPERIMENTS ON FLUIDIZED-BED BIOFILM REACTORS

L. Bignami*, B. Eramo*, R. Gavasci*,
R. Ramadori** and E. Rolle***

**Department of Hydraulic Engineering, University La Sapienza,
Rome, Italy*

***Water Research Institute, CNR, Via Reno 1, 00198 Rome, Italy*

****Department of Chemistry, University La Sapienza, Rome, Italy*

ABSTRACT

Over the last few years considerable attention has been devoted to biological fluidized-bed technology which seems to be potentially more advantageous than both dispersed biomass processes and fixed bed systems. An obstacle to the spreading of this technology is the lack of rigorous criteria in designing reactors, due to the poor knowledge of interconnections of fluid-dynamic aspects with kinetic ones.

This paper reviews the rational basis for reactor design and reports on the experimental tests carried out in order to gain a better understanding in the areas of biofilm modelling and fluidization mechanics.

In particular a biofilm model, in the general case of the Michaelis and Menten equation, was developed and its validity was verified utilizing experimental data obtained in nitrifying batch tests. As to fluidization mechanics the experimental work confirms the Wen and Yu (1966) approach to correlate the bed porosity with the superficial liquid velocity.

KEYWORDS

Fluidized-bed bioreactor; biofilm model; Michaelis and Menten kinetics; fluid-dynamics behaviour; bed porosity; superficial liquid velocity.

INTRODUCTION

All the modern "high-rate" processes are based on some mode of bacterial sludge immobilization achievable either through attachment to high-density particulate carrier materials (immobile support:- fixed or expanded beds; particles in free motion:- fluidized beds) or the formation of highly settleable sludge aggregates.

Each of the high-rate processes has its own specific merits and limitations. Over the last few years considerable attention has been devoted to biological fluidized-bed technology which actually combines the best features of activated sludge and trickling filtration into one process (Stathis, 1980).

The basic concept of the process consists of pushing wastewater upwards through a bed of media such as sand, at velocities sufficient to expand the bed and result in a fluidized state. Once fluidized, the media provide a large surface area for biological growth, which

results in a biomass concentration of approximately one order of magnitude greater than that normally maintained in a suspended growth reactor. This allows much higher loading rates to be used. Moreover, compared with the activated sludge system, the attached biological mass gives the process operator greater stability in handling shock loads and toxic loadings.

Other advantages of fluidized beds are the absence of the clogging and channelling often experienced in fixed beds and, unlike trickling filtration, a minimal biomass sloughing with consequently the virtual absence of biomass wash-out.

A large variety of wastewaters have been investigated on both laboratory- and pilot-scale using biological fluidized-bed technology; the most likely areas for applications are the biological denitrification of river water prior to potable water treatment, the anaerobic treatment of municipal and industrial wastewater, and the upgrading of existing overloaded municipal wastewater treatment plants (Shieh and Keenan, 1986).

This paper presents a theoretical review of the development of a rational model for process design and reports on the experimental tests carried out in order to gain a better understanding of the fluid-dynamic and kinetic factors affecting process performance.

THEORETICAL CONSIDERATIONS

The modelling approach commonly used for heterogeneous catalytic processes is employed in order to obtain a total model for process design.

In essence, the model comprises the following two elements:

- A biofilm model which describes the rate of substrate conversion for individual bioparticles by considering extra-biofilm diffusion and transport of substrate within the biofilm with simultaneous biochemical conversion by microorganisms attached to individual fluidized support particles.
- A fluid-dynamical model which comprises both the analysis of fluidization mechanics and the flow-reactor model; the former describes the degree of bed expansion under a given set of operating conditions (flowrate, biofilm thickness, media size and density, etc.), using the solid-fluid principles; the latter characterizes the liquid phase transport of substrate through a fluidized-bed biofilm reactor. Fluid-dynamical analysis also allows the kinetic significance of transport of substrate from the bulk liquid to the liquid-biofilm interface (external mass transfer) to be evaluated.

The equations obtained from the biofilm model and the fluid-dynamical model define the total model for process design.

The input information required for model application includes:

- the kinetic parameters related to biochemical conversion and internal mass transfer (since only dispersed data are available in literature, the kinetic parameters should be determined experimentally);
- the operating parameters (flowrate and influent/effluent substrate concentrations);
- the biofilm physical parameters (density and moisture content);
- the liquid physical parameters (density and viscosity).

Design parameters to be selected are media size and density, and biofilm thickness; the last variable can be maintained at the desired value through control of the expanded bed height, via biomass wasting.

The sensitivity analysis of the total model (Shieh *et al.*, 1981) verifies that these controllable variables are the most important operating parameters affecting process performance. Under given conditions optimal values of these three parameters exist such that the substrate conversion rate is maximized and the reactor volume requirement is consequently minimized. An iterative procedure utilizing the total model can therefore be followed in order to select parameter values for optimal design (Shieh *et al.*, 1982).

OBJECTIVES

Although a rational and reliable basis for fluidized-bed reactor design can be set up, a comprehensive model requires a better understanding of fluid-dynamic behaviour and a more complete elaboration of the biofilm sub-model related to individual bioparticles.

In particular this work sets out to verify the following aspects related to the model development.

- Biofilm model: up to now the formulation of this model for spherical bioparticles has been accomplished by assuming intrinsic first or zero order kinetics; a more accurate model capable of solving the general case of the Michaelis and Menten equation, is to be set up in order to answer also the questions related to reactor optimization (Andrews and Trapasso, 1985).
- Fluidization mechanics: so far fluid-dynamical analysis has been somewhat neglected despite the fact that it may sometimes decide the success or failure of the process. In particular, two different approaches can be used for predicting the fluid-dynamical behaviour of a biological fluidized bed, based respectively on
 - the force balance for a single isolated particle suspended in a fluid, taking into account bioparticle interaction through inclusion of a correction factor dependent on bed porosity,
 - the empirical Richardson-Zaki relationship (1954), widely used to correlate the bed porosity with the superficial liquid velocity.

Additional fluidization experimentation to compare the two approaches and refine the existing knowledge on the subject is, in any case, required.

EXPERIMENTAL WORK

Biofilm Model

The details of the biofilm model developed have been presented elsewhere (Beccari et al., 1988) and will be briefly summarized here. The model assumptions are:

- steady state conditions;
- spherical support media;
- homogeneous biofilm of uniform thickness;
- the values of biokinetic and diffusivity parameters are constants within the biofilm;
- no external diffusion resistances;
- the substrate considered in the model must be both flux limiting and biokinetically limiting (Williamson and McCarty, 1976);
- Michaelis and Menten type reaction.

With these assumptions, the bioparticle continuity equation for the limiting substrate, S can be written as:

$$\frac{D}{R} \frac{d}{dR} \left(R \frac{dS}{dR} \right) = k \rho \frac{S}{K_s + S} \quad (1)$$

where D is the substrate diffusion coefficient, R is the generic radius, k is the maximum substrate utilization rate, ρ is the biofilm density and K_s is the half velocity coefficient.

The boundary conditions are: $S = S_b = S_s$ at $R = R_p$ and $dS/dR = 0$ (with $S_i > 0$) at $R = R_m$ in the case of full penetration (see curve 1 in Fig. 1), or $S = S_b = S_s$ at $R = R_p$ and $dS/dR = 0$ (with $S_i \approx 0$) at $R = R_m$ in the case of partial penetration (see curve 2 in Fig. 1).

The integration of equation 1 is possible only through numerical methods (Runge-Kutta, Hamming etc.) which, however, require a knowledge of the S concentration and the S gradient at the same R value. In the present case the concentration profile of limiting substrate inside the biofilm can be determined only with the shooting method (a tentative computer solution).

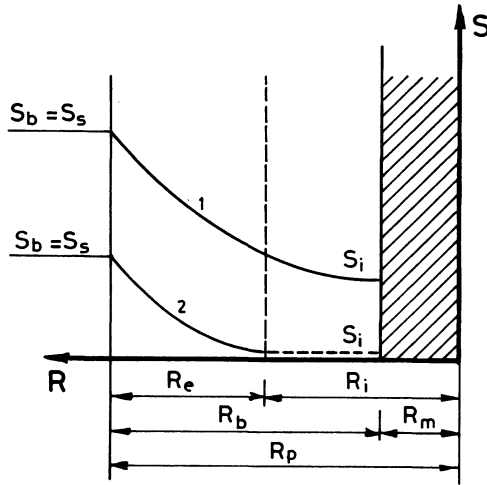


Fig. 1 Concentration profile of limiting substrate inside the biofilm in the case of full penetration (curve 1) and in the case of partial penetration (curve 2): S_b = bulk liquid substrate concentration; S_s = liquid-biofilm interface substrate concentration; S_i = biofilm-support media interface substrate concentration; R_p = bioparticle radius; R_m = support media radius; R_b = biofilm thickness; R_e = active biofilm depth; R_i = inactive radius.

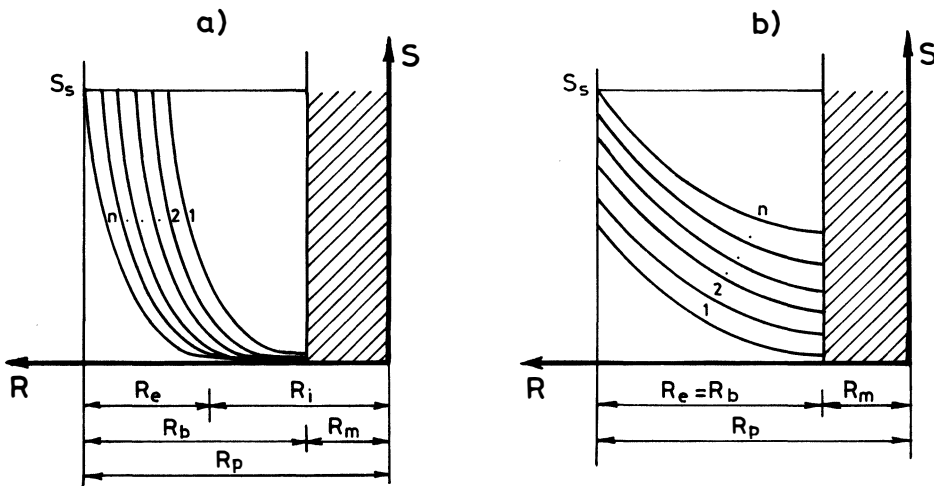


Fig. 2 Search for a solution that verifies the boundary condition.
a) partial penetration of substrate; b) full penetration of substrate.

More specifically the procedure adopted is as follows:

- verify the condition that the same substrate is both flux and biokinetically limiting;
- ascertain input parameters: k , K_s , D , q , R_m , R_b , S_s ;
- set the initial conditions for the first integration: $S = S_i$ and $dS/dR = 0$ at $R = R_m$ (initial S_i is chosen on the basis of the minimum value between $K_s/10$ and $S_b/100$);
- the first numerical integration is continued until one of the two following conditions is achieved: $S = S_s$ at $R < R_p$ (Fig 2a - partial penetration case: curve 1) or $S < S_s$ at $R = R_p$ (Fig. 2b-full penetration case: curve 1);
- in both cases the integration is repeated with new initial conditions. In the partial penetration case $S = S_i$ and $dS/dR = 0$ at R values progressively higher than R_m until a certain value of R (i.e. R_i) is reached for which, at the end of integration, it results that $S = S_s$ at $R = R_p$ (curves from 2 to n in Fig. 2a). In the full penetration case S is taken to be progressively higher than initial S_i , and $dS/dR = 0$ at $R = R_m$ until a certain value of S (i.e. S_i) is reached for which, at the end of integration, it results, that $S = S_s$ at $R = R_p$ (curves from 2 to n in Fig. 2b).

With the concentration profile determined as previously reported, the substrate removal rate referring to a single bioparticle, W , can be obtained from:

$$W = 4\pi R_p J_s \quad (2)$$

where J_s is the flux of limiting substrate in the bioparticle as obtained from:

$$J_s = D \left(\frac{dS}{dR} \right)_{R=R_p} \quad (3)$$

The effectiveness factor, η , defined as the ratio between the actual substrate removal rate and the intrinsic one, is given by:

$$\eta = \frac{W}{q k \frac{S_b}{K_s + S_b} \frac{4}{3} \pi (R_p - R_m)} \quad (4)$$

It is important to note how, also in activated sludge processes, the biological kinetics, as obtained from experimental data, can be lower than the intrinsic ones owing to internal diffusion resistances (Finstein and Heukelekian, 1967; La Motta and Shieh, 1979; Beccari et al. 1985). As the model developed can be applied also to the process with suspended biomass (in this case $R_m = 0$), it has been possible to verify the model utilizing the experimental data obtained in nitrifying batch tests performed with bioflocs having two different media sizes (40 and 80 μm).

The experimental conditions were such that the oxygen was both flux and biokinetically limiting and no significant external diffusion resistances occurred. Oxygen was plotted against time using a particularly accurate technique (Ramadori et al., 1980).

On the assumption that the tests with the 40 μm -flocs were not effected by internal diffusion resistances (La Motta and Shieh, 1979) it has been possible to calculate the intrinsic kinetic parameters, the knowledge of which allows the 80 μm -flocs experimental tests to be simulated.

In the present case it was also necessary to consider the whole period of each test as a train of discrete time intervals, Δt , in which the steady-state conditions have been assumed. In other words it has been hypothesized that during these Δt the S_b remain constant, as well as the profile concentration inside the biofloc. So the substrate removal rate, W , can be calculated for every Δt , for each biofloc present in the reactor. The total substrate removal in the reactor during Δt is simply derived from the sum of the removal rates for every particle. The lower the Δt value assumed, the lower is the error associated with the theoretical determination of S_b pattern vs time.

The measurement of floc size distribution and mean floc volume, V_p , allows the number of

bioflocs, NTP, to be calculated:

$$NTP = VX/Vp\rho \quad (5)$$

where V is the reactor volume, X is the experimentally measured biomass concentration in the reactor and ρ is the biofloc density as it results from literature (Shieh and Keenan, 1986). For the sake of example, the comparison between the experimental data and the model simulation curves referring to a single test is reported in Fig. 3. The two simulation curves show the results obtained using the intrinsic kinetic parameters derived from the $40\mu\text{m}$ -floc test ($k = 7.03 \pm 0.16 \text{ mg O}_2/\text{mg SS d}$; $K_s = 0.65 \pm 0.19 \text{ mg O}_2/\text{l}$). In order to evaluate the model sensitivity for different values used for kinetic parameters, two theoretical curves have been calculated for each test considered. The first one (curve b in Fig. 3, faster kinetic) is characterized by the higher k value combined with the smaller K_s value, while the second one (curve a in Fig. 3, slower kinetic) has the lower k associated with the higher K_s . The validity of the model developed results from the examination of Fig. 3 in which, although the simulation of the batch test can be subject to significant error, good agreement is found between theoretical curves and experimental data. In fact, the model has to predict the substrate curves versus time of Fig. 3 only from the knowledge of the initial substrate concentration. Therefore the divergence between the theoretical curve and experimental data is increased by the sum of the errors made during the repeated application of the model in every single time step (Δt).

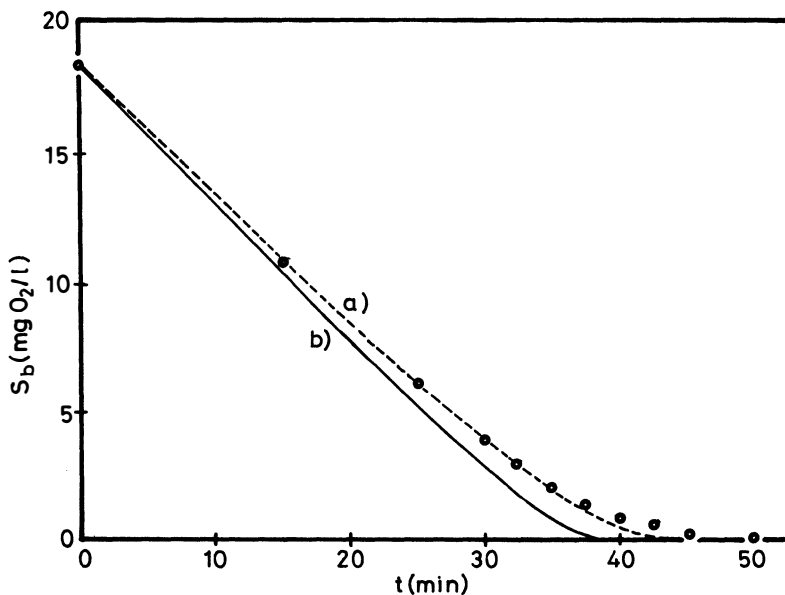


Fig. 3 Pattern of the dissolved oxygen concentration (DO) versus time: comparison between experimental data and the model simulation.
 Experimental working condition:
 $\text{NH}_4\text{-N} = 100 \text{ mg/l}$; $\text{DO (at } t=0) = 18.34 \text{ mg/l}$; mean diameter of bioflocs = $81.45 \mu\text{m}$; $X = \text{MLSS} = 109.7 \text{ mg/l}$.
 Curve a: slower kinetic $k = 6.87 \text{ mg O}_2/\text{mgSS d}$; $K_s = 0.83 \text{ mg O}_2/\text{l}$
 Curve b: faster kinetic $k = 7.18 \text{ mg O}_2/\text{mgSS d}$; $K_s = 0.46 \text{ mg O}_2/\text{l}$.

Moreover, the results have to be considered positively also in view of the fact that the tests were performed with small-size flocs. In these conditions the internal concentration gradients are low and errors can occur during application of the shooting method.

The simulation of experimental tests with the biofilm model also allows the verification of the assumption that the tests with 40 μm -flocs are not affected by internal diffusion resistances.

The theoretical oxygen concentration profiles in 32.6 and 81.2 μm -size flocs and the corresponding effectiveness factors for different oxygen bulk liquid concentrations are reported in Fig. 4 a and b. For the 32.6 μm -flocs the internal concentration is nearly the same as the bulk liquid concentration and the effectiveness factor is higher than 0.98 also for bulk liquid concentrations comparable with the K_s value.

In the case of 81.2 μm -floc (i.e. a size usually found in activated sludge reactors) it can be seen that the internal diffusion resistances become significant ($\eta < 0.9$) only for oxygen bulk liquid concentrations comparable with the K_s value.

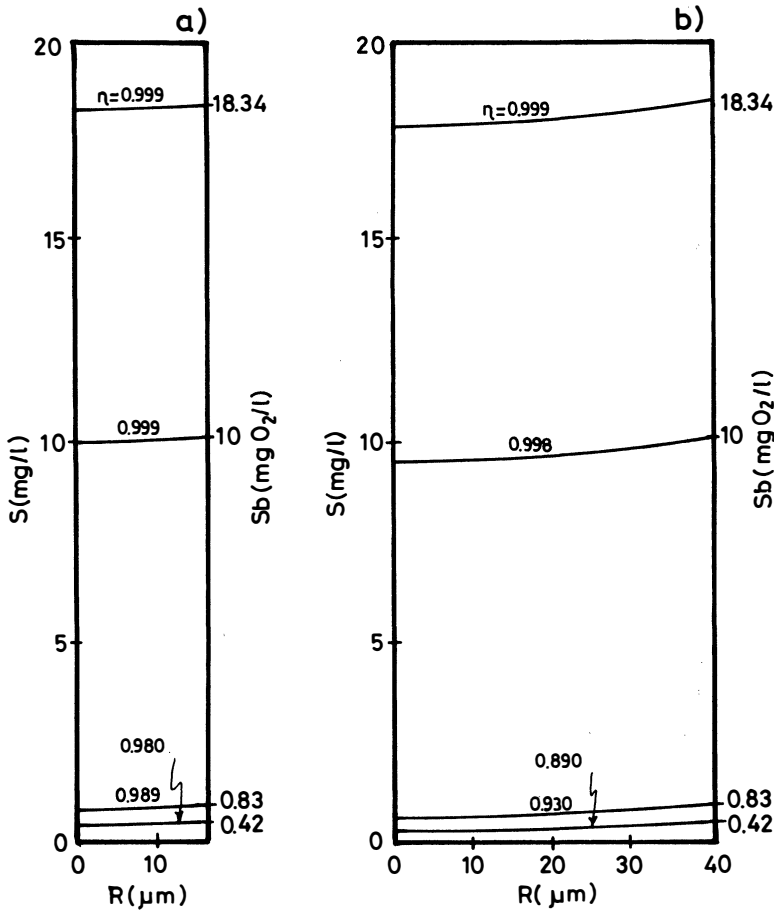


Fig. 4 Theoretical oxygen concentration profile inside 32.6 μm (a) and 81.2 μm (b) size flocs and the corresponding effectiveness factors for different oxygen bulk liquid concentrations.

Bioflocs characteristics: $k = 6.87 \text{ d}^{-1}$, $K_s = 0.83 \text{ mg O}_2/\text{l}$, $D = 2 \text{ cm}^2/\text{d}$, $q = 60 \text{ mg}/\text{cm}^2$

Fluidization mechanics

An initial contribution to the study of this topic is given below in the form of an experimental analysis of the behaviour of beds made up of particles with different shapes and sizes. A comparison is also made with results obtained using expressions normally available in literature.

The experiments were carried out by means of a three-section glass reactor with an internal diameter of ID = 80 mm and a total length of 2280 mm.

Glass and quartz particles having density of 2.916 and 2.640 kg/m³ respectively were used. Table 1 shows the size distribution of the materials utilized, as determined by screenings.

TABLE 1 Size distribution of Glass and Quartz Particles(Percentage)

Opening (mm)	DISTRIBUTION %		
	Glass	Quartz 1	Quartz 2
1.190	15.9		
1.000	63.4		
0.840	20.1		
0.590	0.6		74.2
0.420			25.5
0.297		18.9	0.3
0.149		76.6	
0.105		3.4	
0.074		1.1	

The results obtained are shown in Figs. 5&6. In detail, Fig. 5 shows that the experimental values of the head losses fit the theoretical ones quite well; no channelling phenomena are evident.

Fig. 6 gives the bed porosity (ϵ) as a function of the upflow velocity (v).

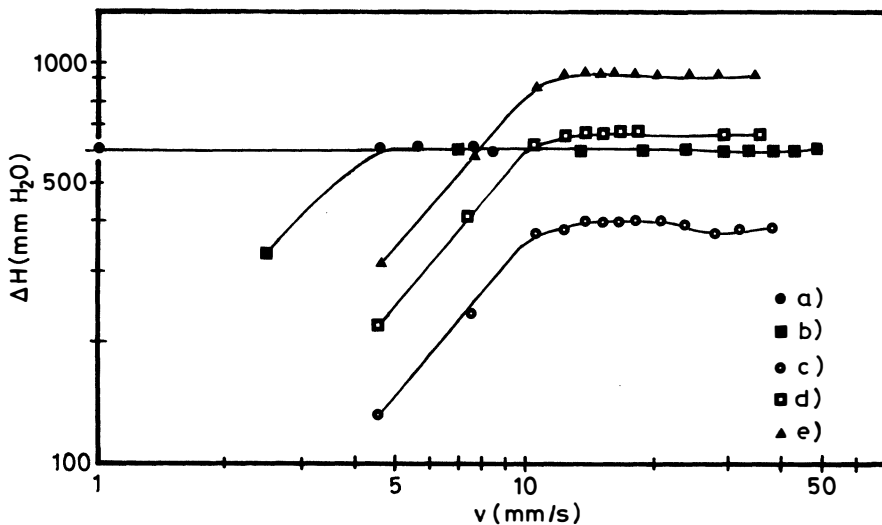


Fig. 5 Head losses in fluidized beds.

- a) Quartz 1; b) Quartz 2;
- c) Glass 3 kg; d) Glass 5 kg;
- e) Glass 7 kg.

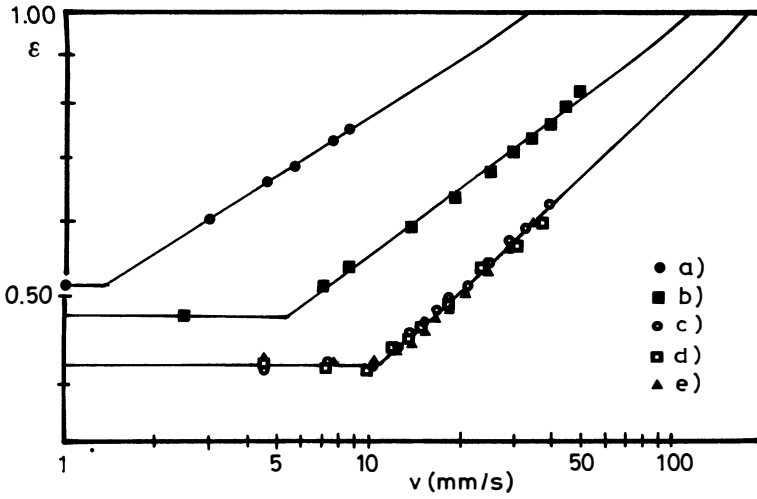


Fig. 6 Bed porosity versus velocity.
 a) Quartz 1; b) Quartz 2;
 c) Glass 3 kg; d) Glass 5 kg;
 e) Glass 7 kg.

From the slopes of the straight lines reported in Fig. 6 the coefficient n of Richardson-Zaki equation (1954) was calculated. Fig. 7 shows the values of n as a function

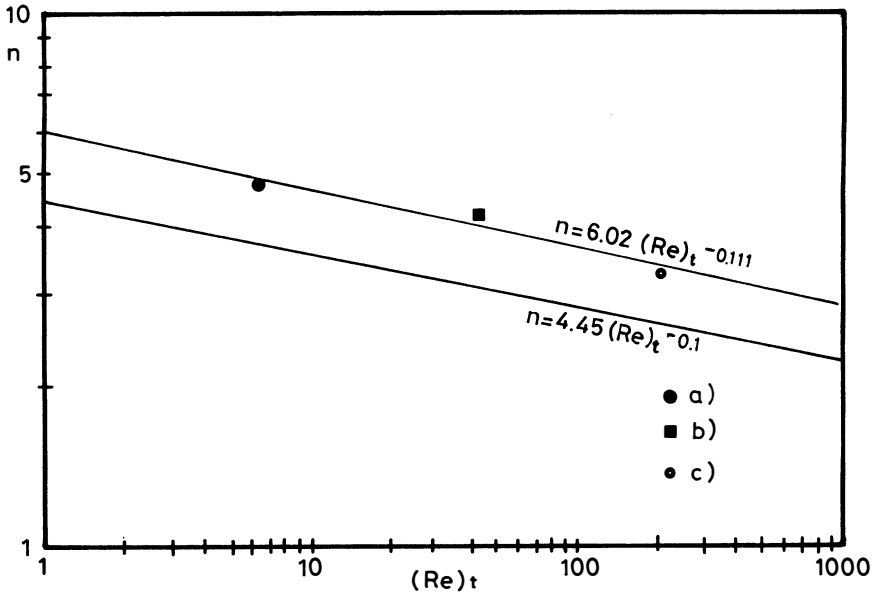


Fig. 7 Expansion index n versus terminal Reynolds number.
 a) Quartz 1; b) Quartz 2; c) Glass

of the terminal Reynolds number (upper curve). A least-squares analysis of the data gives the following correlation:

$$\dot{n} = 6.02 (\text{Re})_t^{-0.111} \quad (6)$$

where (Re) is the Reynolds number corresponding to the settling velocity of a sphere with a diameter D_r , according to Kunii and Levenspiel (1977).

It can be observed that this relationship is significantly different from that one proposed by Richardson and Zaki (1954) in the same range of Reynolds numbers (6 - 210):

$$n = 4.45 (\text{Re})_t^{-0.1} \quad (\text{lower curve in Fig. 7}) \quad (7)$$

The same data were processed also following the Wen and Yu approach (1966):

$$\frac{\text{Ga}}{18 \text{Re} + 2.7 \text{Re}^{1.687}} = f(\varepsilon) \quad (8)$$

where Ga is the Galileo number, Re is the Reynolds number corresponding to the effective fluidization velocity and $f(\varepsilon)$ a factor taking into account the particle interaction. The $f(\varepsilon)$ relation (solid line in Fig. 8):

$$f(\varepsilon) = \varepsilon^{-4.943} \quad (9)$$

is not significantly different from the one by Wen and Yu (dotted line in Fig. 8):

$$f(\varepsilon) = \varepsilon^{-4.7} \quad (10)$$

Preliminary tests were also performed using bioparticles consisting of denitrifying biomass

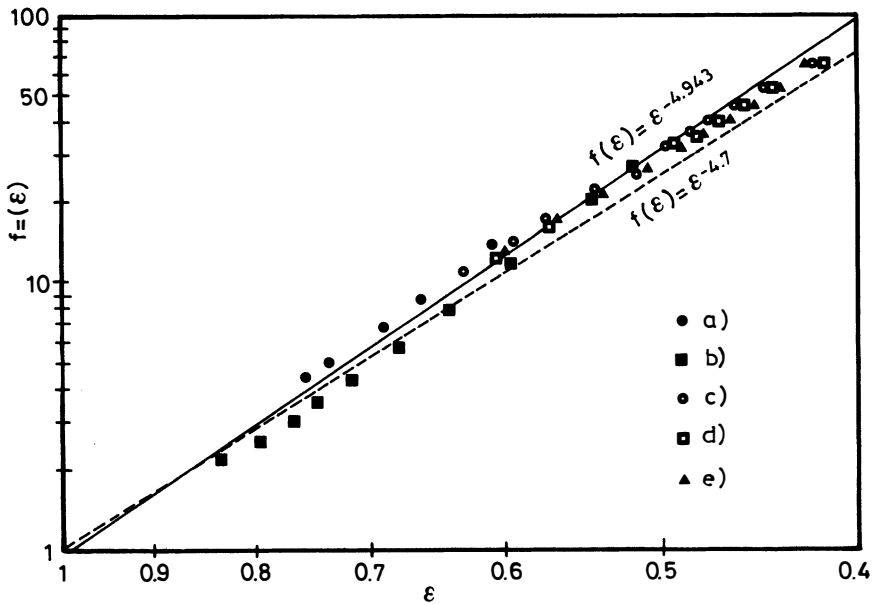


Fig. 8 Voidage function versus bed porosity for rigid particles.

- a) Quartz 1; b) Quartz 2;
- c) Glass 3 kg; d) Glass 5 kg;
- e) Glass 7 kg.

growing on a support medium made up by glass spheres measuring between 1.000 and 1.190 mm in diameter and with a density of 2.916 kg/m^3 .

A sample of the bed was periodically drawn off to measure the geometric and physical characteristics of the bioparticles.

Fig. 9 shows the results elaborated according to the Wen and Yu approach.

The comparison between Fig. 8 and Fig. 9 shows that the slope of the curve referring to the rigid particles is lower (in absolute value) than the ones referring to the bioparticles. In these cases, it must be remarked that the slope appears to be dependent on the biofilm thickness.

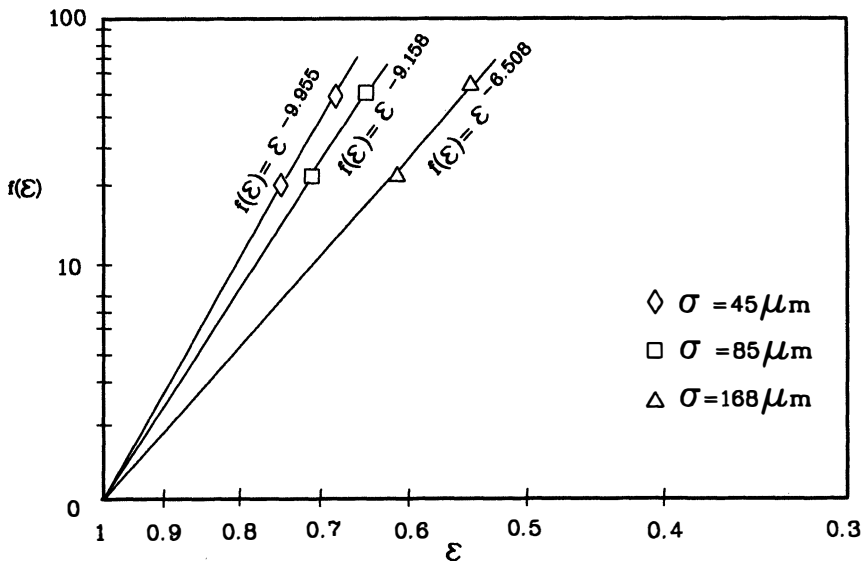


Fig. 9 - Voidage function versus bed porosity for different size bioparticles.

CONCLUSION

In recent years there has been growing interest in the use of fluidized-bed bioreactors in the field of water and wastewater treatment.

This paper shows that there is much need to gain a better understanding of some aspects of process design, in particular in the areas of biofilm modelling and fluidization mechanics. In this regard laboratory-scale experiments have led to the following conclusions.

- The biofilm model developed herein is based on an iterative computer solution and is capable of predicting with reasonable accuracy the relationship between substrate concentration and depth within the biofilm in the general case of the Michaelis and Menten equation without requiring any limiting assumptions regarding reaction order.
- The Wen and Yu correlation, rather than the Richardson and Zaki equation, appears to be a more reliable method for describing the behaviour of fluidized-bed biofilm reactors.

REFERENCES

- Andrews, G. and Trapasso, R. (1985). The optimal design of fluidized bed bioreactors. Journal WPCF, 57, 143-150.
- Beccari, M., Franzini, M. and Ramadori, R. (1985). Effect of diffusion resistances on the kinetics of ammonia oxidation in suspended growth reactors. Paper presented at the workshop on Advanced Biological Processes, CNR Roma 28-30 Novembre 1985. Quaderno n. 77 Istituto di Ricerca sulle Acque pag. 29-46.
- Beccari, M., Bignami, L., Di Pinto, A.C. and Ramadori, R. (1988). Kinetic model of substrate uptake by biofilm in a fluidized bed bioreactor. Sent to Journal WPCF, December 1988.
- Finstein, M.S. and Heukelekian, H. (1967). Gross dimension of activated sludge flocs with reference to bulking. Journal WPCF, 39, 33-40.
- Kunii, D. and Levenspiel, O. (1977). Fluidization Engineering, Robert E., Krieger Publishing Company Huntington.
- La Motta, E.J. and Shieh, W.K. (1979). Diffusion and reaction in biological nitrification. Journal of the Env. Eng. Div., 105, 655-673.
- Ramadori, R., Rozzi, A. and Tandoi, V., (1980). An automated system for monitoring the kinetics of biological oxidation of ammonia. Water Research, 14, 1555-1557.
- Richardson, J.F., Zaki, W.N. (1954). Sedimentation and fluidization: part. I. Trans. Instn. Chem. Engrs., 32, 35-53.
- Shieh, W.K., Sutton, P.M. and Kos, P. (1981). Predicting reactor biomass concentration in a fluidized-bed system. Journal WPCF, 53, 1574-1584.
- Shieh, W.K., Mulcahy, L.T. and La Motta, E.J. (1982). Mathematical model for the fluidized bed biofilm reactor. Enzyme Microb. Technol., 4, 269-275.
- Shieh, W.K. and Keenan, J.D. (1986). Fluidized bed biofilm reactor for wastewater treatment. Adv. in Biochem. Eng. Biotec., 33, 131-169.
- Stathis, T.C. (1980). Fluidized bed for biological wastewater treatment. Journal of the Env. Eng. Div., 106, 227-241.
- Wen, C.Y. and Yu Y.H. (1966). Mechanics of fluidization. Chem. Eng. Prog. Symp. Ser., 62, 100-111.
- Williamson, K. and Mc Carty, P.C. (1976). A model of substrate utilization by bacterial films. Journal WPCF, 48, 9-23.